

Diffusion of rubidium atoms in PDMS thin films

M.J. Kasprowicz^{a,b}, T. Dohnalik^{a,b}, L. Jozefowski^{a,b}, K. Rubahn^a, H.-G. Rubahn^{a,*}

^a *Fysisk Institut, Syddansk Universitet, Campusvej 52, DK-5230 Odense M, Denmark*

^b *Marian Smoluchowski Institute of Physics, Jagiellonian University, Reymonta 4, 30-059, Poland*

Received 11 February 2004; in final form 30 April 2004

Available online 18 May 2004

Abstract

The diffusion coefficient for rubidium in poly-(dimethylsiloxane) thin films has been determined via pulsed laser depletion and cw laser time-of-flight detection of desorbing atoms. The value of the diffusion coefficient of $1.2 \pm 0.7 \times 10^{-5}$ cm²/s agrees with a theoretical estimate and is an important quantity for a quantitative understanding of dynamic light-induced atom desorption.

© 2004 Elsevier B.V. All rights reserved.

1. Introduction

Light-induced atom desorption (LIAD) [1,2] results in a huge, light-induced emission of atoms from thin organic films which cover the inner surface of a glass cell. It is an interesting class of photodesorption in which adsorption–desorption processes from the gas phase to a thin polymeric layer on a glass surface as well as diffusion processes of atoms inside the polymer play an important role. LIAD is a non-thermal phenomenon and can be observed using very low intensity light. It has been observed using Na [1,3], Rb [2,4], K [1] or Cs atoms as well as Na₂ molecules [2]. The organic films used to obtain this effect are for example made of poly-(dimethylsiloxane) (PDMS), octamethylcyclotetrasiloxane (OCT) or paraffines.

Whereas the original LIAD effect has been observed and investigated under equilibrium conditions in glass cells, recently laser-induced desorption of atoms has also been observed under non-equilibrium conditions from PDMS covered glass plates in a high-vacuum apparatus using a pulsed (7 ns) Nd:YAG laser [5–7]. Time-of-flight (TOF) measurements have been used to obtain information about the kinetic energies of the desorbing Na atoms.

The kinetic energies are rather high and show characteristics of both direct electronic excitation (DIET) and phonon assisted desorption. One might speculate that the short pulse length of the desorbing laser selects a certain class of atoms and obscures others, namely low kinetic energy atoms. Hence for comparison we present in this Letter TOF measurements of laser-induced desorption of Rb from PDMS thin films in a high-vacuum apparatus using desorption lasers with short (7 ns) and significantly longer (100 ns) pulse lengths. The resulting desorption yield as a function of laser irradiation time shows depletion characteristics of the sample volume. From yield measurements as a function of time delay between depletion pulses we deduce the diffusion coefficient of Rb atoms in PDMS applying Fick's second law [8,9]. Our experimental value of this coefficient is compared to a theoretical estimate on the basis of molecular dynamics simulations [10].

We note that the diffusion coefficient of alkali atoms in PDMS is an important quantity since it determines the efficiency of atom release from a given desorption spot. Its knowledge will help to quantitatively simulate the LIAD process both under equilibrium and non-equilibrium conditions. This in turn might help to build a very efficient, light-driven source of alkali atoms, which could lead to the construction of a new type of magneto-optical trap [11] for non-stable alkali atoms such as francium.

* Corresponding author. Fax: +45-6615-8760.

E-mail address: rubahn@fysik.sdu.dk (H.-G. Rubahn).

2. Experimental setup

Thin films of PDMS have been generated by covering microscope glass slides with a 10% solution of PDMS in ether using spin-coating at 5000 rpm (rounds per minute). Afterwards the slides have been heated for five hours at 120 °C. This procedure results in a thin ($\approx 1 \mu\text{m}$ thick) rather rough layer of PDMS, which is chemically bound to the underlying glass substrate [6,12,13]. Loading of the PDMS covered plates with alkali metals and desorption experiments were performed in a two-chamber high vacuum apparatus, the two chambers being connected by a magnetically coupled transfer system. In the first chamber a reservoir with a natural mixture of Rb atoms was placed and heated to 75 °C, which results in a Rb partial pressure of 4×10^{-5} mbar [14]. Due to partial adsorption on the stainless steel chamber walls, the partial Rb pressure at the sample place is expected to be of the same order of magnitude as that in a PDMS coated glass cell equipped with a room temperature Rb reservoir (2.4×10^{-7} mbar). The PDMS coated glass slides were placed in this loading vacuum chamber (base pressure $p \approx 5 \times 10^{-7}$ mbar) for a few days. Afterwards the valve to the Rb reservoir was closed, and the Rb filled sample was transported to the main chamber, where the desorption measurements were performed. In the main chamber the sample was transferred on a rotatable manipulator and the valve to the loading chamber was closed so as to ensure a vacuum of $p \approx 4 \times 10^{-9}$ mbar during desorption experiments.

The desorbing light pulses were generated either by a 7 ns, 5 Hz Nd:YAG-laser working at 1064 nm or by a 100 ns KGdWO₄-laser [15], working at 1067 nm. The maximum fluence applied to the samples was in both cases limited to $\approx 400 \text{ mJ/cm}^2$ in order to avoid destruction of the glass surface via color center generation. In most cases the irradiance was even further restricted. Nevertheless irradiation of the PDMS by the pulsed laser resulted in luminescence which appeared in the TOF spectra as an exponentially decaying signal at short flight times. Since the temporal position of this signal was very different from the signal induced by the desorbed atoms it could easily be subtracted from the real TOF spectrum.

Desorbed atoms were detected by their fluorescence, which was induced by a focussed probe beam. Online/offline measurements and the use of the two-chamber apparatus with initially no Rb in the desorption chamber made sure that the observed TOF signals resulted solely from Rb atoms desorbed from the sample plate. The probe beam was produced by a Littrow configuration diode laser (Sacher Lasertechnik), tuned to the Rb⁸⁵ D₁ line at 794.5 nm, corresponding to the Doppler broadened hyperfine transitions $F = 3 \rightarrow F' = 2$ and $F = 3 \rightarrow F' = 3$. The geometrical configuration of the laser beams in the high-vacuum chamber is shown in

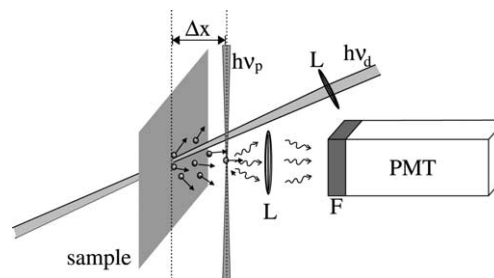


Fig. 1. Sketch of the detection system: $h\nu_p$ – probe beam; $h\nu_d$ – desorption beam; L – lenses; F – filter; PMT – photomultiplier tube.

Fig. 1. The desorbed atoms traversed the focused detection beam, where they were excited to an upper electronic level. Photons from the resulting spontaneous emission back to the ground state were imaged by collection optics to the cathode of a photomultiplier. Interference filters ($\lambda_1 = 787 \pm 7.5 \text{ nm}$ and $\lambda_2 = 810 \pm 15.5 \text{ nm}$) were used to reduce the noise level of the signal, induced by background light. Since exciting and emitted photons have the same frequencies, minimization of reflected light from the exciting laser was essential. To achieve that goal we inserted Brewster-angle windows at the entrance and at the exit of the diode laser into the vacuum apparatus, thus reducing greatly reflections inside the chamber.

Time-of-flight measurements were performed with the help of a multichannel analyzer (box sizes from 10 to 80 ns) which temporarily correlated the desorption laser pulse with the arrival time of the desorbed atoms within the focus of the detection beam. The distance Δx between the detection focal point and the spot of the desorbing laser was 9 mm. The temporal resolution for thermal atoms was of the order of 1 μs due to the finite diameter of the detection laser beam.

3. Results and discussion

Fig. 2 shows typical TOF data obtained by the use of two different desorption lasers. The peak positions of both signals are within measurement uncertainty identical although the measurements were done on different days after different durations of previous light illumination of the sample. The peak position did also not shift with changing the desorption laser fluence. Hence the most probable kinetic energies of the desorbed atoms, $E_{\text{mp}} = 200 \pm 70 \text{ meV}$, are independent of pulse length of the desorption laser and also of prehistory of the samples. The slightly different behaviour of the TOF curves at longer flight times (i.e., lower kinetic energies) is assigned to slightly different positions of the desorption lasers with respect to the detection laser. In fact, since the detection laser results in a detection line rather than a detection point, the flight time is less well defined,

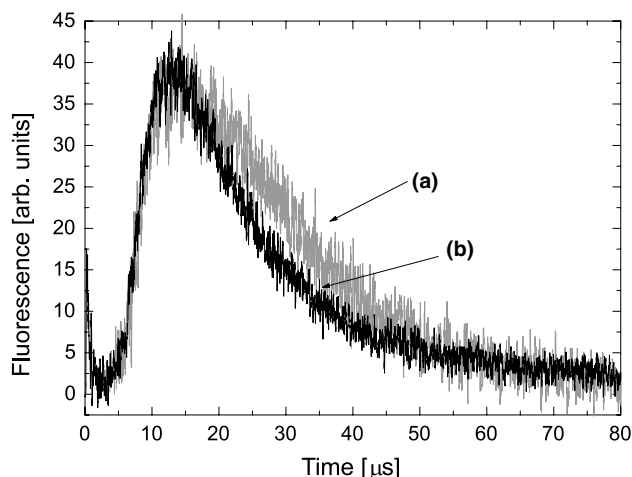


Fig. 2. Typical TOF signals obtained by the use of desorption lasers with different pulse lengths: (a) 7 ns Nd:YAG-laser (fluence 240 mJ/cm²); (b) 100 ns KGdWO₄-laser (fluence 120 mJ/cm²). Time-of-flight distance $\Delta x = 9 \pm 1$ mm.

thus resulting in a broadening of the TOF peaks to longer flight times. For that reason we concentrate our discussion on the peak position, which is rather unaffected by this smear-out.

With increasing irradiation time during a measurement the signal intensity of desorbed atoms decreased. Repeated measurements without transferring the sample into the loading chamber decreased this intensity, too (cf. Fig. 3a vs. 3b). Longer deposition times of Rb in the samples did not result in larger signals, but delayed this attenuation process, i.e., allowed more measurements to be made before the Rb was totally depleted from the PDMS. However, keeping the sample in the dark between measurements resulted in an increase of signal intensity (Fig. 3c). Since there is no external Rb reservoir in the desorption chamber, this is a clear hint for dif-

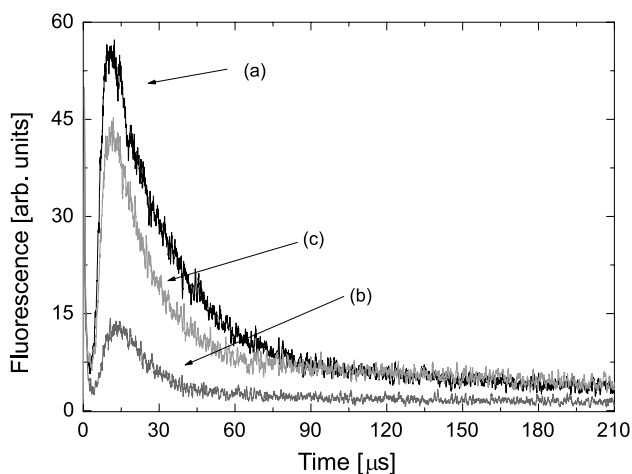


Fig. 3. TOF signal after: (a) 100 s irradiation; (b) 1200 s irradiation with the Nd:YAG-laser. The signal (c) has been obtained after 3 h break without illumination.

fusion out of the non-irradiated area of the PDMS film as the source for desorbed atoms.

In order to obtain a value of the diffusion coefficient of Rb in PDMS, we have applied a fixed number of pulses (500) from the infrared laser to desorb atoms from the desorption laser spot on the sample surface. The irradiation of PDMS will lead to a local heating, the energy of which, however, is transferred mainly into kinetic energies of the desorbed atoms [7]. A heating effect on the measured diffusion coefficient can be excluded since we are measuring the diffusion after the desorption laser has been turned off. The total flux of desorbed rubidium was measured by integrating the one-photon laser-induced fluorescence signal over a fixed time interval. Following a delay time Δt a second series of pulses was used to desorb atoms which have undergone diffusional motion from the surrounding areas into the desorption area. The delay time was then varied and the experiment repeated.

Fig. 4 shows the resulting normalized integrated desorption intensities as a function of Δt . Normalization has been performed by dividing the integrated signal intensities at given delay time $\Delta t \neq 0$ by that obtained at delay time $\Delta t = 0$. Since it was not possible to perform reliable measurements for integration times below 100 s we have not obtained data points for Δt much smaller than 100 s.

The diffusion coefficient can be obtained by fitting the time-dependent desorption signal from diffusional refilling according to

$$S(t) = 1 - 2 \int_0^\infty \frac{J_1^2(ua)}{u} \exp(-D\Delta t u^2) du, \quad (1)$$

where a is the radius of the circular desorption spot, J_1 is a Bessel function and D is the diffusion coefficient. In our experiment, the radius of the desorbing laser spot a

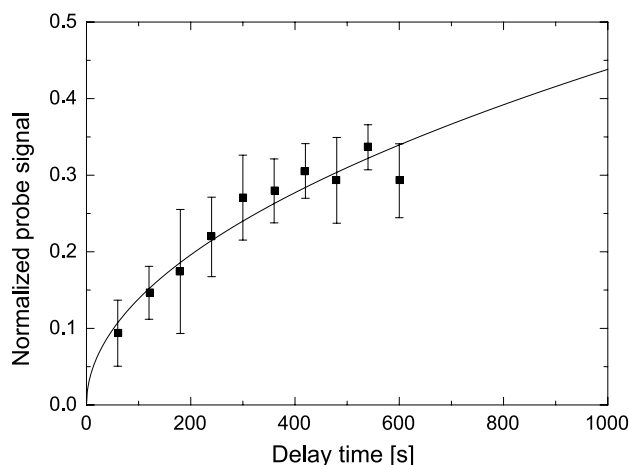


Fig. 4. Experimental data for diffusion of rubidium in PDMS. Normalized probe signal $S(t)$ is the integrated desorption intensity following a given time delay divided by the initial desorption intensity. The line is a fit using Eq. (2).

was 2 ± 0.5 mm. The large uncertainty in this value takes into account that the intensity distribution in the desorption spot is not perfectly hat-shaped. In the limit of small desorption flux, Eq. (1) can be approximated by [16,17]

$$S(t) \approx (2/a)\sqrt{D\Delta t/2\pi}. \quad (2)$$

Since we obtain even after prolonged irradiation an atomic flux from the initial desorption spot, the small desorption flux limit is fulfilled.

We have fitted Eq. (2) to our results (Fig. 4) and have obtained $D = (1.2 \pm 0.7) \times 10^{-5}$ cm²/s. Here, the uncertainty is due to the desorption laser geometry, the ill defined detection point and the short flight path of the desorbed atoms. Unfortunately, the limited thickness of the organic film as well as its sensitivity to radiation damage makes it difficult to improve the measurement accuracy.

We note that the measured diffusion coefficient describes both the dark diffusion along and normal to the polymer surface, D_0 , and the diffusion in the presence of light, $D(\lambda)$. It has previously been argued [4] that this latter contribution gives rise to a square root dependence of the total desorption yield as a function of fluence of the irradiating light in the case of atom desorption inside closed gas cells. Since the kinetic energies of the desorbed atoms seem to follow a resonant heating mechanism [7] one might interpret the dependence of the diffusion coefficient on the light power as a local temperature dependence.

Let us compare the measured diffusion coefficient with a theoretical prediction from Molecular Dynamics simulations of diffusional gas transport through PDMS [10]. This classical mechanics simulation implements for the two-body bonded interactions in PDMS as well as for the non-bonded interactions between the foreign particles and PDMS Lennard–Jones (LJ) potentials with LJ parameters σ which are given approximately by the diameter of the foreign particles. The diffusion coefficient D_0 is calculated for various embedded atoms and molecules. It is shown that D_0 decreases exponentially with increasing σ . Since no calculations for Rb in PDMS have been performed, we have to estimate the theoretical value of D_0 by assuming a LJ parameter. We take $\sigma \simeq 3.7$ Å since this is the equilibrium ground state separation of Rb₂ [18]. For this value the theoretical diffusion coefficient is $(0.8 \pm 0.2) \times 10^{-5}$ cm²/s, which agrees within errors with our measurements.

We note that the experimentally observed enhancement of the diffusion rate by the laser light cannot be simply described by assuming that in the presence of light we are talking about diffusion of an electronically excited particle. The internuclear distance of the first

excited states of Rb₂ is approximately 5 Å [18]. This would result in a diffusion coefficient of $D \approx 0.1 \times 10^{-5}$ cm²/s, i.e., smaller than the coefficient for ground state Rb₂. However, the Molecular Dynamics simulations in [10] are performed for simple ground state interaction potentials, and thus more sophisticated calculations are asked for a thorough comparison between experiment and theory.

Acknowledgements

M.K. acknowledges the financial support provided through the European Community's Human Potential Programme under contract HPRN-CT-2002-00304, FASTNet. We are grateful to the Danish Research Agency SNF and to NATO via a CLG Grant 979024 for further support. We thank V.G. Bordo, L. Moi, A. Burchianti, C. Marinelli and E. Mariotti for stimulating discussions.

References

- [1] A. Gozzini, F. Mango, J.H. Xu, G. Alzetta, F. Maccarrone, R.A. Bernheim, *NuovoCimento D* 15 (1993) 709.
- [2] M. Meucci, E. Mariotti, P. Bicchi, C. Marinelli, L. Moi, *Europhys. Lett.* 25 (1994) 639.
- [3] J.H. Xu, A. Gozzini, F. Mango, G. Alzetta, R.A. Bernheim, *Phys. Rev. A* 54 (1996) 3146.
- [4] S.N. Atutov, V. Biancalana, P. Bicchi, C. Marinelli, E. Mariotti, M. Meucci, A. Nagel, K.A. Nasyrov, S. Rachini, L. Moi, *Phys. Rev. A* 60 (1999) 4693.
- [5] J. Brewer, Master Thesis, University of Southern Denmark, 2003.
- [6] J. Brewer, A. Burchianti, C. Marinelli, E. Mariotti, L. Moi, K. Rubahn, H.-G. Rubahn, *Appl. Surf. Sci.* 228 (2004) 40.
- [7] J. Brewer, V.G. Bordo, M.J. Kasprovicz, H.-G. Rubahn, *Phys. Rev. A* 69 (2004) 000.
- [8] S.M. George, A.M. DeSantolo, R.B. Hall, *Surf. Sci. Lett.* 159 (1985) L425.
- [9] R. Viswanathan, D.R. Burgess Jr., P.C. Stair, E. Weitz, *J. Vac. Sci. Technol.* 20 (1982) 605.
- [10] R.M. Sok, PhD Thesis, University of Groningen, 1994.
- [11] S.N. Atutov, R. Calabrese, V. Guidi, B. Mai, A.G. Rudavets, E. Scansani, L. Tomassetti, V. Biancalana, A. Burchianti, C. Marinelli, E. Mariotti, L. Moi, S. Veronesi, *Phys. Rev. A* 67 (2003) 053401.
- [12] T. Mundry, Heat curing siliconization of pharmaceutical glass containers, PhD Thesis, Humboldt University Berlin, 1999.
- [13] K. Rubahn, J. Ihlemann, G. Jakopic, A.C. Simonsen, H.-G. Rubahn, *Appl. Phys. A* (accepted).
- [14] A.N. Nesmeyanov, *Vapor Pressure of the Chemical Elements*, Elsevier, Amsterdam, 1963.
- [15] K.A. Stankov, G. Marowsky, *Appl. Phys. B* 61 (1995) 213.
- [16] E. Rideal, J. Tadayon, *Proc. Roy. Soc. (London)* A225 (1954) 357.
- [17] J. Crank, *The Mathematics of Diffusion*, second edn., Oxford University Press, London, 1975.
- [18] C. Amiot, *J. Chem. Phys.* 93 (1990) 8591.